Multi-shell diffusion models improve white matter characterization in cerebral small vessel disease

Marek J. Konieczny[1,*], MSc, Anna Dewenter[1,*], MSc, Annemieke ter Telgte[2], MSc,

Benno Gesierich[1], PhD, Kim Wiegertjes[2], MSc, Sofia Finsterwalder[1], MSc, Anna Kopczak[1], MD,

Mathias Hübner[1], MSc, Rainer Malik[1], PhD, Anil M. Tuladhar[2], MD, PhD,

José P. Marques[3], PhD, David G. Norris[3], PhD, Alexandra Koch[4], PhD, Olaf Dietrich[5], PhD,

Michael Ewers[1], PhD, Reinhold Schmidt[7], MD, Frank-Erik de Leeuw[2], MD, PhD,

Marco Duering[1,2,8], MD

[1] Institute for Stroke and Dementia Research (ISD), University Hospital, LMU Munich, Germany

[2] Department of Neurology, Donders Institute for Brain, Cognition and Behaviour, Radboud
   University Medical Center, Nijmegen, The Netherlands

[3] Radboud University, Donders Institute for Brain, Cognition, and Behavior, Nijmegen, The
   Netherlands

[4] Population Health Sciences, German Center for Neurodegenerative Diseases (DZNE), Bonn,
   Germany

[5] Department of Radiology, University Hospital, LMU Munich, Germany

[7] Medical University of Graz, Department of Neurology, Graz, Austria

[8] Munich Cluster for Systems Neurology (SyNergy), Munich, Germany

*these authors contributed equally as first authors

Search terms: [2] All Cerebrovascular disease/Stroke; [27] CADASIL; [32] Vascular

dementia; [120] MRI; [128] DWI

Submission Type: Article

Title character count: 99

Number of references: 40

Number of tables: 4

Number of figures: 3

Word count abstract: 282

Word count paper: 4285

Supplement data is available from Zenodo (Table e-1): https://doi.org/10.5281/zenodo.3908176

Corresponding Author:

Marco Duering

Institute for Stroke and Dementia Research

Klinikum der Universität München

Feodor-Lynen-Str. 17, 81377 Munich, Germany

T: +49-89-4400-46166

E: marco.duering@med.uni-munchen.de

Statistical Analyses performed by:

Marek J. Konieczny, Benno Gesierich

Author Disclosures:

AnK reports travel grants from Pfizer Pharma GmbH, unrelated to this work. MD reports honoraria for lectures from Bayer Vital GmbH and Pfizer Pharma GmbH, unrelated to this work. All other authors report no disclosures.

ABSTRACT

Objective: To test the hypothesis that multi-shell diffusion models improve the characterization of microstructural alterations in cerebral small vessel disease (SVD), we assessed associations with processing speed performance, longitudinal change and reproducibility of diffusion metrics.

Methods: We included 50 sporadic and 59 genetically defined SVD patients (CADASIL) with cognitive testing and standardized 3T MRI, including multi-shell diffusion imaging. We applied the simple diffusion tensor imaging (DTI) model and two advanced models: diffusion kurtosis imaging (DKI) and neurite orientation dispersion and density imaging (NODDI). Linear regression and multivariable random forest regression (including conventional SVD markers) were used to determine associations between diffusion metrics and processing speed performance. The detection of short-term disease progression was assessed by linear mixed models in 49 sporadic SVD patients with longitudinal high-frequency imaging (in total 459 MRIs). Inter-site reproducibility was determined in 10 CADASIL patients scanned back-to-back on two different 3T MRI scanners.

Results: Metrics from DKI showed the strongest associations with processing speed performance (R^2 up to 21%) and the largest added benefit on top of conventional SVD imaging markers in sporadic SVD and CADASIL patients with lower SVD burden. Several metrics from DTI and DKI performed similarly in detecting disease progression. Reproducibility was excellent (intraclass correlation coefficient > 0.93) for DTI and DKI metrics. NODDI metrics were less reproducible.

Conclusion: Multi-shell diffusion imaging and DKI improve the detection and characterization of cognitively relevant microstructural white matter alterations in SVD. Excellent reproducibility of diffusion metrics endorses their use as SVD markers in research and clinical care. Our publicly available inter-site dataset facilitates future studies.

Classification of Evidence: This study provides Class I evidence that in patients with SVD, diffusion MRI metrics are associated with <mark>processing speed</mark> performance.

INTRODUCTION

Cerebral small vessel disease (SVD) is the most important vascular contributor to cognitive decline and dementia.[1] There is a great need for accessible, clinically relevant and reproducible biomarkers of the disease.[2] MRI is the method of choice for diagnosis and monitoring disease progression.[3] While MRI findings also include visible tissue lesions – such as white matter hyperintensities (WMH), lacunes, microbleeds and brain atrophy – recent work converges on the high potential of diffusion imaging metrics as markers for SVD.[4-7] Diffusion metrics typically outperform conventional SVD imaging markers in explaining clinical deficits and in detecting disease progression, while also enabling a high grade of automation.[4]

Diffusion tensor imaging (DTI) is a well-established technique to quantify microstructural white matter alterations. However, the tensor model oversimplifies diffusion processes and more advanced models were introduced to better take into account the complexity of white matter.[8,9] While these new methods may be more suited to characterize microstructural tissue alterations in SVD, they require more elaborate MRI acquisition in form of multi-shell diffusion imaging (i.e. using more than one diffusion weighting). The added benefit of multi-shell diffusion imaging and advanced diffusion modelling in SVD is so far largely unexplored. In addition, little is known about the inter-site reproducibility of diffusion metrics in SVD patients, which is considered a roadblock for application in multicenter studies and clinical routine.

The aim of this study was to evaluate two advanced multi-shell diffusion models, diffusion kurtosis imaging (DKI) and neurite orientation dispersion and density imaging (NODDI), in comparison with DTI. We combined a sporadic SVD sample and a genetically defined sample

(Cerebral Autosomal Dominant Arteriopathy with Subcortical Infarcts and Leukoencephalopathy, CADASIL) for independent validation. In terms of biological validity, we hypothesized that advanced diffusion metrics are more strongly associated with processing speed deficits, the main and often only cognitive deficit in SVD, and improve the monitoring of disease progression. To address instrumental validity, we determined inter-site reproducibility of diffusion metrics.

METHODS

Study participants

For the analysis of sporadic SVD patients (cross-sectional and longitudinal), we used data from the RUN DMC – InTENse study (Radboud University Nijmegen Diffusion tensor and Magnetic resonance imaging Cohort – Investigating The origin and EvolutioN of cerebral small vessel disease). Details of the study protocol have been published.[10,11] In short, this study included 54 patients from the previous RUN DMC study with a high likelihood of progression of SVD while excluding individuals with other stroke etiologies. All 54 patients were invited to baseline MRI assessment and in total 9 monthly follow-up MRI scans. For the cross-sectional analysis we used data from the baseline visit. Two patients had to be excluded due to highly enlarged ventricles resulting in substantial CSF contamination in the white matter skeleton, and two patients because of confounding of neuropsychological tests (e.g. through the presence of an arm paresis), which resulted in a final sample of 50 sporadic SVD patients. Data from all MRI sessions (baseline and up to 9 follow-ups) were used for the longitudinal analysis. A few visits had to be excluded from the longitudinal analysis due to insufficient data quality (n = 3). 5 out of the 54 patients were excluded from the longitudinal analysis due to a low number of follow-up visits (≤ 2). The final sample for the longitudinal analysis included 49 patients with a median of 9 (range 4 -10) MRIs per patient (in total 459 MRI scans).

CADASIL patients for the cross-sectional validation analysis were recruited through the ongoing VASCAMY study (Vascular and Amyloid Predictors of Neurodegeneration and Cognitive Decline in Nondemented Subjects) in Munich.[4,12] The CADASIL diagnosis was confirmed by either molecular genetic testing (cysteine-altering *NOTCH3* mutation) or by skin biopsy (presence of granular osmiophilic material). 3 patients had to be excluded due to insufficient MRI

quality. The final validation sample comprised 59 CADASIL patients. For the inter-site reproducibility study, 10 CADASIL patients underwent MRIs on two different 3T MRI scanners within 24 hours.

Standard Protocol Approvals, Registrations, and Patient Consents

Study protocols were approved by the local ethics committee of the respective institution. Written informed consent was obtained from all patients.

Cognitive and clinical characterization

Across both samples, neuropsychological and clinical assessment was performed following identical protocols. For cognitive characterization, we a priori focused on processing speed as the core deficit in SVD, which frequently occurs isolated, i.e. without impairment in other cognitive domains.[12-14] To reduce the number of statistical tests, we pre-specified to analyze only processing speed, assessed by the time to complete Trail Making Test matrix A and B. We calculated an established compound score by averaging age- and education-corrected z-scores for matrix A and B.[12] The z-score transformation was based on healthy subjects from the literature.[15] In addition, patients were characterized with regard to vascular risk factors (arterial hypertension, hypercholesterolemia, diabetes, smoking status), activities of daily living (Barthel Index), focal neurological symptoms (National Institutes of Health Stroke Scale), and disability (modified Rankin scale). The latter two scales were available for CADASIL patients only.

MRI acquisition and conventional SVD imaging markers

MRI scans were performed on 3 Tesla scanners (sporadic SVD: Magnetom Prisma with 32-channel head coil; CADASIL: Magnetom Skyra with 64-channel head/neck coil; Siemens Healthineers, Erlangen, Germany). Protocols in both studies included a 3D T1, 3D fluid-attenuated inversion recovery (3D-FLAIR), 3D gradient echo (T2*-weighted), and multi-band echo planar imaging multi-shell diffusion-weighted imaging (MS-DWI) sequences (sporadic SVD / CADASIL: repetition time 3220 / 3800 ms, echo time 74 / 105 ms, diffusion-encoding directions 30 ($b = 1000$ s/mm^2) and 60 ($b = 3000$ / 2000 s/mm^2, 10 $b = 0$ images, multi-band factor 3). One $b = 0$ image with inverted phase-encoding direction was acquired for correction of susceptibility-induced distortions during processing. A complete description of all sequence parameters is available from Zenodo (**Table e-1**): https://doi.org/10.5281/zenodo.3908176.

For the inter-site reproducibility analysis, 10 CADASIL patients were scanned on two different 3T scanners (Siemens Magnetom Skyra and Siemens Magnetom Prisma, both with 64-channel head/neck coil) using a diffusion imaging protocol harmonized in terms of resolution, b-values and diffusion-encoding directions. Differences in the gradient system resulted in longer repetition and echo times on the Skyra system. While the two scanners were both in Munich, they were located in separate buildings and operated independently, which is why we consider this an inter-site study.

Conventional SVD imaging markers (WMH volume, lacune volume, microbleed count, brain volume) were quantified according to consensus criteria.[3] All volumes were normalized to intracranial volume. Details on the calculation of conventional SVD imaging markers have been described previously.[4,11]

Diffusion MRI preprocessing

Preprocessing steps included visual quality control, denoising, Gibbs artefact removal, and

correction for susceptibility-induced distortions, eddy current-induced distortions, as well as head

motion. This was done using tools from MRtrix3 (http://www.mrtrix.org/, dwidenoise,

mrdegibbs)[16] and the Functional Magnetic Resonance Imaging of the Brain (FMRIB) Software

Library (FSL; version 5.0.10, topup, eddy).[17]

Diffusion models and metrics

We included 12 diffusion metrics from the following diffusion models: diffusion tensor imaging

(DTI), diffusion kurtosis imaging (DKI) and neurite orientation dispersion and density imaging

(NODDI). DTI metrics were calculated using 'dtifit' in FSL (using only $b = 0$ and $b = 1000$

s/mm^2 images),[17] DKI metrics using the Diffusional Kurtosis Estimator

(http://www.nitrc.org/projects/dke)[18] and NODDI metrics using the NODDI Matlab toolbox

(http://www.nitrc.org/projects/noddi_toolbox).[9] For DTI, we calculated fractional anisotropy,

mean diffusivity, axial diffusivity and radial diffusivity. For DKI, we calculated kurtosis

fractional anisotropy, mean kurtosis, axial kurtosis and radial kurtosis. For NODDI, we

calculated neurite density index, orientation dispersion index, extracellular volume fraction and

cerebrospinal fluid volume fraction, which are the most commonly used NODDI metrics. The

modeled diffusion properties or microstructural tissue features presumably represented by these

different metrics are listed in **Table 1**.

Diffusion metrics were analyzed within major white matter tracts. For this purpose, we applied

the tract-based spatial statistics pipeline in FSL[17] to skeletonize the diffusion data. Registrations

to standard space and projections onto the white matter skeleton were estimated from fractional

anisotropy images and then applied to all other diffusion metrics. We used a custom mask to

exclude all areas typically susceptible to cerebrospinal fluid partial volume effects, a critical step when analyzing patient samples with brain atrophy.[4] To obtain global diffusion metrics, we averaged the values of the diffusion metrics across the entire skeleton. For regional associations, we performed voxel-wise analyses (see below).

Statistical analysis

Statistical analyses were performed using R (version 3.2.4).[19] Comparisons of sample characteristics between sporadic SVD and CADASIL patients were performed with t-tests or non-parametric Wilcoxon rank sum tests for numeric variables and Fisher exact test for categorical variables.

Since SVD burden was much higher in CADASIL patients and to facilitate a comparison to sporadic SVD patients, we pre-defined a sensitivity analysis in a subgroup of CADASIL patients with lower SVD burden, i.e., CADASIL patients with WMH volume below the third quartile (WMH volume <Q3, n = 44).

Three analyses were conducted to assess how well the metrics from the different diffusion models explain cognition in sporadic SVD and CADASIL patients.

First, we determined for each diffusion metric the association with the age- and education-corrected processing speed compound score using linear regression analysis. For this purpose, the processing speed compound scores were power-transformed in both samples using the Yeo-Johnson transformation[20] to approximate normal distribution.

Second, we assessed the added benefit of each diffusion metric for predicting processing speed on top of conventional SVD imaging markers, i.e. WMH volume, lacune volume, microbleeds, and brain volume. Given the presence of intercorrelations between all imaging markers we deployed random forest regression, which offers increased robustness against multicollinearity

when using conditional inference trees (R package 'party').[21] We constructed one random forest

regression model with conventional SVD imaging markers only, and 12 more models including

in addition each diffusion metric. Prediction accuracy was calculated for each random forest

regression model as the root-mean-square error (RMSE) between observed and predicted values

using leave-one-out cross-validation. The added benefit of each diffusion metric for prediction of

processing speed was quantified by the difference in RMSEs between models with and without

diffusion metric. We repeated random forest regression 100 times to determine the point estimate

and a 95% confidence interval for the RMSE.

Third, we looked into regional associations between diffusion metrics and processing speed using

voxel-wise regression analyses in sporadic SVD. Since SVD is a pathology affecting the entire

white matter, including normal-appearing white matter, and processing speed is regarded as a

global network function, we considered a higher number of significant voxels as favorable. We

used permutation test theory with a standard general linear model as implemented in 'randomise'

(FSL), with 5000 permutations and threshold-free cluster enhancement with $p < 0.01$, corrected

for multiple comparisons.

To assess the potential added value of combining diffusion metrics, we performed a principal

component analysis using the R function 'prcomp' ('stats' package) without specifying the

maximal rank. The first two principal components were included in an additional linear

regression and random forest regression analysis as described above.

To assess the ability of diffusion metrics to capture disease progression over time in sporadic

SVD, we estimated linear mixed models, one for each diffusion metric. A model for WMH

volumes was added for comparison. We assumed a continuous progression of SVD over the 10

months studies, which can be captured by a linear mixed model. Time of MRI visits (relative to

baseline visit) was modeled as fixed effect, including a random intercept and slope for each

subject. The fixed effect corresponds to the mean change in the diffusion metric over time, while accounting for patient-specific variability. Marginal R^2 represents the variance explained by the fixed effect. Before estimation of linear mixed models, diffusion metrics and WMH volumes were normalized individually for each subject to the baseline score and then centered and scaled (by subtracting the mean and dividing through the standard deviation). This resulted in standardized fixed effects expressed as change in standard deviations per time unit (i.e. week). The following R packages were used for estimation of linear mixed models: 'lme4' (version 1.1-21)[22], 'lmerTest' (version 3.1.0)[23], 'boot' (version 1.3-22)[24], 'MuMIn' (version 1.43.6)[25]. To determine the reproducibility of diffusion metrics across MRI scanners we calculated intraclass correlation coefficients with the R package 'psych' (1.8.12)[26] and applied the one-way ANOVA model, i.e. intraclass correlation coefficient (1,1).[27]

Data availability

Anonymized data will be made available upon request to the corresponding author.

RESULTS

Sample characteristics are presented in **Table 2**. Compared with sporadic SVD patients,

CADASIL patients were younger, had higher SVD burden and more severe processing speed

impairment.

Associations of global diffusion alterations with processing speed

We first assessed associations between global diffusion metrics and processing speed, the main

cognitive deficit in SVD (**Figure 1**). In sporadic SVD, we found the strongest associations for

DKI metrics (mean kurtosis and axial kurtosis, both R^2 = 18%), which explained more variance

than the best performing DTI metric (axial diffusivity, R^2 = 12%). NODDI metrics also showed

strong associations with processing speed (extracellular volume fraction, R^2 = 18%). Validation

analysis in the CADASIL sample showed in general higher explained variances, but effect sizes

for most metrics were similar (R^2 ranging from 23% to 28%). In the pre-specified sensitivity

analysis of CADASIL patients with lower SVD burden (WMH volume <Q3), the strongest

association with processing speed was found for radial kurtosis (R^2 = 20%). Similar to the

sporadic SVD sample, DKI metrics explained more variance (R^2 = 21-27%) than the best

performing DTI metric (fractional anisotropy, R^2 = 14%). Of note, orientation dispersion index

from the NODDI model was the only diffusion metric not showing a significant association with

processing speed in all samples.

Next, we compared the added benefit of diffusion metrics on top of conventional SVD markers

(WMH volume, lacune volume, microbleeds, brain volume) for predicting processing speed

performance. In sporadic SVD patients, most metrics (except for fractional anisotropy,

orientation dispersion index and cerebrospinal fluid volume faction) showed an added benefit

(**Figure 1B**). The strongest increase in prediction accuracy was found for radial kurtosis (three times higher than the best performing DTI metric axial diffusivity). A different pattern was found for CADASIL patients. Here, all DTI metrics performed better than metrics from advanced diffusion models, with the strongest increase in prediction accuracy for fractional anisotropy. In CADASIL patients with lower SVD burden (WMH volume <Q3), extracellular volume fraction as well as radial and mean kurtosis were the only diffusion metrics with a significant increase in accuracy on top of conventional SVD markers. In this subgroup, there was no added benefit of DTI metrics.

Combining multiple diffusion metrics using principal component analysis

To test if a combination of diffusion MRI metrics provides additional value in explaining processing speed performance, we first entered all diffusion metrics into a principal component analysis. The first two principal components explained 91% of the variance in sporadic SVD patients, 92% in CADASIL patients and 90% in the CADASIL patients with lower SVD burden (WMH volume <Q3). In linear regression, these two components together performed similar in explaining processing speed (sporadic SVD: R^2 = 19%, CADASIL: R^2 = 31%, CADASIL patients with lower SVD burden: R^2 = 17%; **Figure 1A**) compared with the better performing individual metrics. In random forest regression, the components showed an added benefit in sporadic SVD and CADASIL patients (**Figure 1B**), but this benefit was not higher than that of the best-performing individual diffusion metric. There was no added benefit in CADASIL patients with lower SVD burden.

Associations of regional diffusion alterations with processing speed

We next compared diffusion metrics regarding voxel-wise associations with processing speed.

Metrics from both advanced multi-shell diffusion models showed a very high sensitivity to detect

voxel-wise associations with processing speed, with up to 59% of white matter tract voxels being

significant. The number of significant voxels was substantially lower (up to 16%) for DTI metrics

(**Figure 2, Table 3**).

Longitudinal changes of diffusion metrics in serial imaging during 10 months

We evaluated the ability of diffusion metrics to track short-term changes in tissue microstructure

using the high-frequency, serial MRI data in sporadic SVD patients. Example time-courses for

WMH volumes and one metric from each diffusion model are depicted in **Figure 3A**. Linear

mixed models revealed a significant change over time (fixed effect) for most metrics, including

the conventional SVD imaging marker WMH volume (**Figure 3B**). Metrics from DTI and DKI

performed best as indicated by largest fixed effects and marginal R^2. The performance of DTI

and DKI metrics as judged by effect sizes was overall very similar. NODDI metrics showed

relatively low performance, even lower than that of the conventional SVD imaging marker WMH

volume.

Inter-site reproducibility

To address reproducibility of diffusion metrics, 10 CADASIL patients participated in an inter-site

study using two 3T MRI scanners. These patients were overall comparable in terms of

demographics, clinical scores and SVD burden on MRI to the other CADASIL groups (Table 2).

Diffusion metrics from DTI and DKI showed excellent inter-site reproducibility with intraclass

correlation coefficients above 0.99 for DTI metrics and above 0.93 for DKI metrics (**Table 4**).

Reproducibility of NODDI was overall good for most metrics, but substantially lower in comparison with the other models (intraclass correlation coefficients ranging from 0.26 to 0.94). Scatter plots for NODDI metrics suggest a systematic shift of values between the two MRI sites (**Figure 3C**).

DISCUSSION

We evaluated multi-shell diffusion imaging and advanced diffusion modelling for the characterization of microstructural tissue alterations in SVD. Our main findings are that (1) advanced metrics from DKI and NODDI showed the strongest associations with cognitive deficits in two independent samples; (2) DTI and DKI metrics performed best in detecting short-term disease progression; (3) reproducibility was excellent for DTI and DKI metrics, but not for metrics from the NODDI model. These findings encourage the use of multi-shell diffusion imaging, and in particular DKI, to characterize SVD-related white matter damage in multi-center studies and clinical care.

Metrics from DKI and NODDI performed best in assessing associations between white matter alterations and cognitive deficits, both in the global and the regional (voxel-wise) analysis. They also showed the greatest benefit on top of conventional SVD imaging markers. Interestingly, a combination of diffusion metrics using principal component analysis did not perform better than individual metrics. Radial and mean kurtosis as well as the extracellular volume fraction had the highest added benefit in sporadic SVD patients. Importantly, this finding was independently validated in genetically-defined SVD patients, but only in the pre-specified subgroup of 44 patients with lower SVD burden (WMH volume <Q3). We can thus conclude that multi-shell imaging and advanced diffusion modelling are best suited to characterize early stages of SVD. In early stages tissue alterations can be subtle, especially outside of visible lesions. While it is already established that DTI metrics are altered in the so-called normal-appearing white matter, our results suggest that the advanced models DKI and NODDI are even more suited to characterize these subtle alterations. Current concepts of SVD acknowledge the need for

intervention in early stage patients and advanced diffusion models offer a sensitive tool to characterize these patients.

Others already reported a benefit of advanced models in other conditions, e.g. in assessing gliomas using DKI[28] or describing microstructural changes in ischemic stroke using NODDI.[29] DKI metrics have also been shown to better capture gray matter abnormalities and associations with clinical deficits in patients with multiple sclerosis.[30] Studies in SVD are sparse. One study reported an association between mean kurtosis in the cortex and WMH volume, but kurtosis of the white matter was not assessed.[31] Another group found decreased kurtosis in the white matter of the frontal and parietal lobes in patients with severe leukoaraiosis.[32] However, associations with cognitive performance or longitudinal change were not investigated.

An explanation for the improved performance of the advanced diffusion models DKI and NODDI in assessing brain structure-function relationships might be found in the limitations of the DTI model. The simple tensor model describes diffusion of water molecules using a Gaussian distribution. Due to the complex organization of brain microstructure, the assumption of a Gaussian distribution is typically violated. The DKI model specifically takes this into account by assessing kurtosis, i.e. the deviation from a Gaussian normal distribution. Thus, DKI characterizes tissue complexity, with lower complexity being reflected in lower kurtosis. Interestingly, the DKI model did not perform better than the DTI model in the entire CADASIL sample, which includes patients with very high lesion load. This might indicate that tissue complexity in late disease stages is already reduced to such an extent that modelling Gaussian distribution via DTI is sufficient for quantification.

Apart from serving as markers, diffusion metrics can also provide insights into the underpinnings of tissue alterations. DTI and DKI are sensitive to microstructural alterations, but lack specificity. NODDI aims to directly model microstructural features such as neurite density and neurite orientation dispersion using a multi-compartment model. Interestingly, neurite orientation dispersion, which can reflect demyelination,[33] did not show associations with cognitive deficits or change over time. Among NODDI metrics, we found the best results for the extracellular volume fraction. This is in line with our previous work using a bi-tensor model, in which we showed that diffusion alterations in SVD are driven by an increase of extracellular free water.[34]

The advanced diffusion models come at a relevant cost. The need to acquire multi-shell diffusion data, measuring at multiple and higher diffusion weightings, results in prolonged acquisition times and higher requirements in terms of scanner hardware. The combination of 3T MRI and multi-band imaging, which acquires multiple slices simultaneously (https://www.cmrr.umn.edu/multiband/), overcomes this limitation.[35] Our two-shell acquisition schemes using a multi-band factor of 3 resulted in a scanning time between 7 and 8 minutes for the diffusion sequence, a duration well-suited for clinical routine. Especially the NODDI model might benefit from an even more sophisticated acquisition with more diffusion weightings and directions, but this would in our view have prolonged the scanning time to an extent that would no longer be feasible for clinical routine examinations.

Despite the benefit of advanced diffusion models over DTI in explaining cognitive deficits, we did not see an advantage in tracking of short-term progression in sporadic SVD patients. Radial kurtosis was the only metric from the advanced models that performed as well as tensor metrics in assessing change over time. All other advanced metrics performed worse than DTI and within

the range or even worse than longitudinal WMH measurements. The longitudinal analysis on the high-frequency serial imaging data with its up to 10 monthly measurements can be regarded as an extended scan-rescan study. More stable metrics with less variability from visit to visit allow to better detect change over time. Our data suggests that the advanced models, and especially the NODDI model, result in higher variability. The inter-site study in CADASIL patients, where NODDI metrics showed lower reproducibility than other metrics, points in a similar direction. Overall, one might speculate that the advanced models with their complex algorithms are less robust than the simple DTI model, thus impeding on longitudinal measurements and comparability between sites.

Reproducibility of MRI markers is crucial for multi-center studies and clinical routine, where many different scanners are deployed. Still, inter-site reproducibility studies are rarely conducted, especially in specific patient populations. Both scan-rescan repeatability and inter-site reproducibility of DTI metrics has been shown to be excellent in healthy subjects.[36] To our knowledge, reproducibility of DTI in SVD was so far only assessed in one of our previous studies,[4] however that study was performed across different field strengths. In that previous setting, histogram analysis of mean diffusivity values using PSMD (peak width of skeletonized mean diffusivity) substantially improved reproducibility. Since reproducibility was already excellent for DTI measures in the current study using two scanners with identical field strength and a harmonized acquisition protocol, we did not apply the histogram analysis approach. Fewer reproducibility studies are available for DKI and NODDI. One scan-rescan study investigated kurtosis measures in traumatic brain injury and reported better repeatability than DTI measures.[37] NODDI metrics were shown to be repeatable in a scan-rescan study with healthy volunteers.[38] With a large SVD lesion burden, our CADASIL inter-site sample was markedly

different from previously studied healthy control samples. In the CADASIL sample, reproducibility for NODDI metrics was substantially lower compared to other metrics. These findings illustrate the need to assess reproducibility in the targeted patient population, not only in healthy volunteers. To fill this void and to facilitate future analyses, we made our inter-site dataset publicly available for download (http://intersite.isd-muc.de).

Our study has some potential limitations. We analyzed the diffusion metrics only in relation to processing speed as determined by the Trail Making Test, but no other neuropsychological domain. Since processing speed is the earliest, most pronounced, and often the only cognitive deficit in SVD patients, we decided a priori to focus on processing speed in order to limit the number of statistical tests. Minor differences in scanner types and consequently sequence parameters between the sporadic SVD and CADASIL sample might also be regarded as a limitation, in particular the different repetition and echo times in the inter-site study. However, as illustrated in our inter-site analysis, the reproducibility of most diffusion metrics across scanners was excellent. CADASIL is caused by *NOTCH3* mutations and has a distinct molecular pathophysiology, which is different from sporadic SVD. Still, the clinical presentation, including symptoms, cognitive profile and imaging findings, is remarkably similar, thus validating CADASIL as a model disease for pure SVD.[13,39,40]

Strengths of the study include the use of two independent and complementary SVD samples to assess the relationship between diffusion metrics and processing speed. While data from sporadic SVD patients increases the generalizability of our findings, the younger sample of genetically defined SVD enabled us to study SVD without confounding factors associated with aging. Moreover, we employed random forest regression to account for multicollinearity and linear

mixed models to account for patient-specific variability. Another unique strength is the inter-site

dataset, which we made publicly available.

APPENDIX 1: Authors

Name	Location	Contribution
Marek J. Koniecny, MSc	LMU Munich	Acquisition, statistical analysis and interpretation of data, drafting the manuscript
Anna Dewenter, MSc	LMU Munich	Interpretation of data, drafting and revising the manuscript
Annemieke ter Telgte, MSc	Radboudumc Nijmegen	Study design, acquisition and interpretation of data, revising the manuscript
Benno Gesierich, PhD	LMU Munich	Analysis, statistical analysis and interpretation of data, revising the manuscript
Kim Wiegertjes, MSc	Radboudumc Nijmegen	Acquisition and interpretation of data, revising the manuscript
Sofia Finsterwalder, MSc	LMU Munich	Interpretation of data, revising the manuscript
Anna Kopczak, MD	LMU Munich	Major role in acquisition of data, revising the manuscript
Mathias Hübner, MSc	LMU Munich	Major role in acquisition of data, revising the manuscript
Rainer Malik, PhD	LMU Munich	Interpretation of data, statistical advice, revising the manuscript
Anil M. Tuladhar, MD, PhD	Radboudumc Nijmegen	Interpretation of data, revising the manuscript
José P. Marques, PhD	Donders Institute Nijmegen	MRI protocol design, acquisition of data, revising the manuscript
David J. Norris, PhD	Donders Institute Nijmegen	Interpretation of data, revising the manuscript
Alexandra Koch, PhD	DZNE Bonn	Interpretation of data, revising the manuscript

Olaf Dietrich, PhD	LMU Munich	Acquisition of data, interpretation of data, revising the manuscript
Michael Ewers, PhD	LMU Munich	Interpretation of data, revising the manuscript
Reinhold Schmidt, MD	Medical University Graz	Interpretation of data, revising the manuscript
Frank-Erik de Leeuw, MD, PhD	Radboudumc Nijmegen	Study design and supervision, interpretation of data, revising the manuscript
Marco Duering, MD	LMU Munich	Study concept, design and supervision, acquisition, analysis and interpretation of data, drafting and revising the manuscript

REFERENCES

1. Wardlaw JM, Smith C, Dichgans M. Small vessel disease: mechanisms and clinical implications. Lancet Neurol 2019;18:684-696.

2. Smith EE, Schneider JA, Wardlaw JM, Greenberg SM. Cerebral microinfarcts: the invisible lesions. The Lancet Neurology 2012;11:272-282.

3. Wardlaw JM, Smith EE, Biessels GJ, et al. Neuroimaging standards for research into small vessel disease and its contribution to ageing and neurodegeneration. Lancet Neurol 2013;12:822-838.

4. Baykara E, Gesierich B, Adam R, et al. A Novel Imaging Marker for Small Vessel Disease Based on Skeletonization of White Matter Tracts and Diffusion Histograms. Ann Neurol 2016;80:581-592.

5. Nitkunan A, Barrick TR, Charlton RA, Clark CA, Markus HS. Multimodal MRI in cerebral small vessel disease: its relationship with cognition and sensitivity to change over time. Stroke 2008;39:1999-2005.

6. Patel B, Markus HS. Magnetic resonance imaging in cerebral small vessel disease and its use as a surrogate disease marker. International Journal of Stroke 2011;6:47-59.

7. Zeestraten EA, Benjamin P, Lambert C, et al. Application of Diffusion Tensor Imaging Parameters to Detect Change in Longitudinal Studies in Cerebral Small Vessel Disease. PloS one 2016;11:e0147836.

8. Jensen JH, Helpern JA, Ramani A, Lu H, Kaczynski K. Diffusional kurtosis imaging: the quantification of non-gaussian water diffusion by means of magnetic resonance imaging. Magnetic resonance in medicine : official journal of the Society of Magnetic Resonance in Medicine / Society of Magnetic Resonance in Medicine 2005;53:1432-1440.

9. Zhang H, Schneider T, Wheeler-Kingshott CA, Alexander DC. NODDI: practical in vivo neurite orientation dispersion and density imaging of the human brain. Neuroimage 2012;61:1000-1016.

10. ter Telgte A, Wiegertjes K, Tuladhar AM, et al. Investigating the origin and evolution of cerebral small vessel disease: The RUN DMC – InTENse study. European Stroke Journal 2018;3:369-378.

11. ter Telgte A, Wiegertjes K, Gesierich B, et al. The contribution of acute infarcts to cerebral small vessel disease progression. Ann Neurol 2019.

12. Duering M, Zieren N, Herve D, et al. Strategic role of frontal white matter tracts in vascular cognitive impairment: a voxel-based lesion-symptom mapping study in CADASIL. Brain 2011;134:2366-2375.

13. Charlton RA, Morris RG, Nitkunan A, Markus HS. The cognitive profiles of CADASIL and sporadic small vessel disease. Neurology 2006;66:1523-1526.

14. Zieren N, Duering M, Peters N, et al. Education modifies the relation of vascular pathology to cognitive function: cognitive reserve in cerebral autosomal dominant arteriopathy with subcortical infarcts and leukoencephalopathy. Neurobiol Aging 2013;34:400-407.

15. Tombaugh TN. Trail Making Test A and B: normative data stratified by age and education. Arch Clin Neuropsychol 2004;19:203-214.

16. Tournier JD, Smith R, Raffelt D, et al. MRtrix3: A fast, flexible and open software framework for medical image processing and visualisation. Neuroimage 2019:116137.

17. Smith SM, Jenkinson M, Woolrich MW, et al. Advances in functional and structural MR image analysis and implementation as FSL. Neuroimage 2004;23 Suppl 1:S208-219.

18. Tabesh A, Jensen JH, Ardekani BA, Helpern JA. Estimation of tensors and tensor-derived measures in diffusional kurtosis imaging. Magnetic resonance in medicine : official journal

of the Society of Magnetic Resonance in Medicine / Society of Magnetic Resonance in Medicine 2011;65:823-836.

19. R Core Team. A language and environment for statistical computing. Vienna, Austria: R Foundation for Statistical Computing, 2016.

20. Yeo IK, Johnson RA. A new family of power transformations to improve normality or symmetry. Biometrika 2000;87:954-959.

21. Strobl C, Malley J, Tutz G. An introduction to recursive partitioning: rationale, application, and characteristics of classification and regression trees, bagging, and random forests. Psychol Methods 2009;14:323-348.

22. Bates D, Mächler M, Bolker B, Walker S. Fitting linear mixed-effects models using lme4. arXiv preprint arXiv:14065823 2014.

23. Kuznetsova A, Brockhoff PB, Christensen RHB. lmerTest package: tests in linear mixed effects models. Journal of Statistical Software 2017;82.

24. Canty A, Ripley B. boot: Bootstrap R (S-Plus) functions. R package version 1.3-11. 2014.

25. Barton K, Barton MK. Package 'MuMIn'. Multi-model inference version 2019;1.

26. Revelle WR. psych: Procedures for personality and psychological research. 2017.

27. Shrout PE, Fleiss JL. Intraclass correlations: uses in assessing rater reliability. Psychol Bull 1979;86:420-428.

28. Zhao J, Wang YL, Li XB, et al. Comparative analysis of the diffusion kurtosis imaging and diffusion tensor imaging in grading gliomas, predicting tumour cell proliferation and IDH-1 gene mutation status. J Neurooncol 2019;141:195-203.

29. Wang Z, Zhang S, Liu C, et al. A study of neurite orientation dispersion and density imaging in ischemic stroke. Magn Reson Imaging 2019;57:28-33.

30. Bester M, Jensen JH, Babb JS, et al. Non-Gaussian diffusion MRI of gray matter is associated with cognitive impairment in multiple sclerosis. Mult Scler 2015;21:935-944.

31. Zhong G, Zhang R, Jiaerken Y, et al. Better correlation of cognitive function to white matter integrity than to blood supply in subjects with leukoaraiosis. Frontiers in aging neuroscience 2017;9:185.

32. Xu S, Ye D, Lian T, et al. Assessment of severity of leukoaraiosis: a diffusional kurtosis imaging study. Clinical imaging 2016;40:732-738.

33. Grussu F, Schneider T, Tur C, et al. Neurite dispersion: a new marker of multiple sclerosis spinal cord pathology? Annals of clinical and translational neurology 2017;4:663-679.

34. Duering M, Finsterwalder S, Baykara E, et al. Free water determines diffusion alterations and clinical status in cerebral small vessel disease. Alzheimer's & dementia : the journal of the Alzheimer's Association 2018.

35. Setsompop K, Cohen-Adad J, Gagoski B, et al. Improving diffusion MRI using simultaneous multi-slice echo planar imaging. Neuroimage 2012;63:569-580.

36. Grech‑Sollars M, Hales PW, Miyazaki K, et al. Multi‑centre reproducibility of diffusion MRI parameters for clinical sequences in the brain. NMR in Biomedicine 2015;28:468-485.

37. Kuhn T, Gullett J, Nguyen P, et al. Test-retest reliability of high angular resolution diffusion imaging acquisition within medial temporal lobe connections assessed via tract based spatial statistics, probabilistic tractography and a novel graph theory metric. Brain imaging and behavior 2016;10:533-547.

38. Tariq M, Schneider T, Alexander DC, Wheeler-Kingshot C, Zhang H. Scan-rescan reproducibility of neurite microstructure estimates using NODDI. 2012: The British Machine Vision Association and Society for Pattern Recognition.

39. Wollenweber FA, Baykara E, Zedde M, et al. Cortical Superficial Siderosis in Different Types of Cerebral Small Vessel Disease. Stroke 2017;48:1404-1407.

40. Duering M, Csanadi E, Gesierich B, et al. Incident lacunes preferentially localize to the edge of white matter hyperintensities: insights into the pathophysiology of cerebral small vessel disease. Brain 2013;136:2717-2726.

TABLES

Table 1: Diffusion models and metrics

Model	Metric		Modelled diffusion property/ Microstructural tissue feature
DTI	FA	Fractional anisotropy	Directionality of water diffusion
	MD	Mean diffusivity	Extent of water diffusion
	AD	Axial diffusivity	Extent of water diffusion along the main direction of water diffusion
	RD	Radial diffusivity	Extent of water diffusion perpendicular to the main direction
DKI	KFA	Kurtosis fractional anisotropy	Directionality of kurtosis (i.e. non-Gaussian water diffusion)
	MK	Mean kurtosis	Extent of kurtosis
	AK	Axial kurtosis	Extent of kurtosis parallel to main direction of diffusion
	RK	Radial kurtosis	Extent of kurtosis perpendicular to main direction of diffusion
NODDI	NDI	Neurite density index	Intracellular water content (fraction), modelled as sticks
	ODI	Orientation dispersion index	Angular variation of neurite orientation
	fECV	Extracellular volume fraction	Extracellular water content (fraction), modelled as anisotropic tensor
	fCSF	CSF volume fraction	CSF content (fraction), modelled as isotropic tensor

Abbreviations: CSF = cerebrospinal fluid; DKI = diffusion kurtosis imaging; DTI = diffusion tensor imaging; NODDI = neurite orientation dispersion and density imaging.

Table 2: Sample characteristics

	Sporadic SVD (RUN DMC – InTENse)	CADASIL (all) (VASCAMY)	CADASIL (WMHV <Q3) (VASCAMY)	CADASIL (inter-site)	*p**
n	50	59	44	10	
Demographic characteristics					
Age [years], median (IQR)	68.2 (7.4)	57 (13.5)	54.5 (15.0)	55.5 (13.3)	<0.0001
Female, *n* (%)	18 (36.0)	39 (66.1)	30 (68.2)	5 (50.0)	0.002
Vascular risk factors, *n* (%)					
Hypertension	41 (82.0)	18 (30.5)	15 (34.1)	3 (30.0)	<0.0001
Hypercholesterolemia	25 (50.0)	31 (52.5)	22 (50.0)	5 (50.0)	0.849
Diabetes	5 (10.0)	1 (1.7)	1 (2.3)	0 (0)	0.092
Current or past smoking	37 (74.0)	35 (59.3)	25 (56.8)	3 (30.0)	0.155
Clinical scores, median (IQR)					
Processing speed z-score	-0.15 (1.06)	-0.51 (1.44)	-0.45 (1.06)	-0.13 (0.90)	0.029
Barthel scale score	100 (5)	100 (0)	100 (0)	100 (0)	0.134
NIHSS score	-	0 (0)	0 (0)	0 (0)	-
mRS score	-	0 (1)	0 (0.25)	0 (1)	-
Conventional SVD markers, median (IQR)					
WMHV[a] [%]	0.35 (0.57)	5.34 (4.45)	4.06 (3.75)	7.67 (2.62)	<0.0001
Lacune count	0 (0)	3 (4.5)	2 (4)	3 (7.75)	<0.0001
Lacune volume[a] [10^{-4}]	0 (0)	1.25 (3.84)	0.88 (3.74)	0.99 (2.20)	<0.0001
Microbleed count	0 (1)	3 (6.5)	2 (7.3)	0.5 (1.75)	<0.0001
Brain volume[a] [%]	78.1 (5.34)	75.6 (6.67)	75.5 (5.31)	75.7 (7.03)	0.015

Abbreviations: IQR = interquartile range; mRS = modified Rankin Scale; NIHSS = National Institutes of Health Stroke Scale; WMHV = white matter hyperintensity volume

* Sporadic SVD sample (n=50) vs. CADASIL (all) sample (n=59)
[a] Normalized to the intracranial volume

Table 3: Voxel-wise regressions with processing speed

	DTI				**DKI**				**NODDI**			
	FA	MD	AD	RD	KFA	MK	AK	RK	NDI	ODI	fECV	fCSF
n	0	511	13862	0	0	44290	10611	1501	42799	2671	50574	0
%	0	0	16	0	0	51	12	2	50	3	59	0

n = number of significant voxels (within the white matter skeleton)
% = percentage of significant voxels in relation to all voxels of the white matter skeleton

Table 4: Inter-site reproducibility

	DTI				DKI				NODDI			
	FA	MD	AD	RD	KFA	MK	AK	RK	NDI	ODI	fECV	fCSF
ICC	0.995	0.993	0.992	0.993	0.975	0.985	0.931	0.993	0.942	0.255	0.792	0.808

Abbreviations: ICC = intraclass correlation coefficient.

FIGURE LEGENDS

Figure 1: Associations between global diffusion metrics and processing speed. Analyses were performed in a sporadic SVD sample, a CADASIL sample and a pre-specified subgroup of CADASIL patients with lower SVD burden (white matter hyperintensity volumes below the third quantile; <Q3). (**A**) Linear regressions between each diffusion metric and processing speed. Color depicts explained variance (R^2), circle size depicts p-value. The direction of the association is indicated by plus (positive association) and minus (negative) signs. (**B**) Multivariable random forest regression exploring the added benefit of each diffusion metric on top of conventional SVD markers. Plots indicate point estimate and 95% confidence interval for the change in model accuracy as assessed by the RMSE decrease.

Abbreviations: AD = axial diffusivity; AK = axial kurtosis; DKI = diffusion kurtosis imaging; DTI = diffusion tensor imaging; FA = fractional anisotropy; fCSF = cerebrospinal fluid volume fraction; fECV= extracellular volume fraction; KFA= kurtosis fractional anisotropy; MD = mean diffusivity; MK = mean kurtosis; NDI = neurite density index; NODDI = neurite orientation dispersion and density imaging; ODI = orientation dispersion index; PCs = principal components; RD = radial diffusivity; RK = radial kurtosis; RMSE = root mean squared error.

Figure 2: Associations between regional diffusion metrics and processing speed. For each diffusion model, the metric with the highest number of significant voxels (Table 3) is depicted. Compared with mean diffusivity (MD), mean kurtosis (MK) and extracellular volume fraction (fECV) result in more than twice as many significant voxels (red, after correction for multiple comparisons). L = left.

Figure 3: Disease progression and inter-site reproducibility analysis. (**A**) Single subject data

of sporadic SVD patients plotted against time. WMH volume and one diffusion metric from each

model are shown as examples. For better appreciation of single subject time-courses, five

subjects are highlighted by black lines. Red lines show the fixed effect of time calculated by

linear mixed models. (**B**) Results from linear mixed models: Standardized fixed effects (change

in SD per week ± bootstrapped 95% confidence interval) and marginal R2 (variance explained by

time). *p < 0.05, **p < e-07, ***p < e-09 (**C**) Scatter plots illustrating inter-site reproducibility in

CADASIL patients. In case of perfect agreement between the two MRI scanners, the linear fit

(solid line) would match the dashed diagonal. ICC = intraclass correlation coefficient.
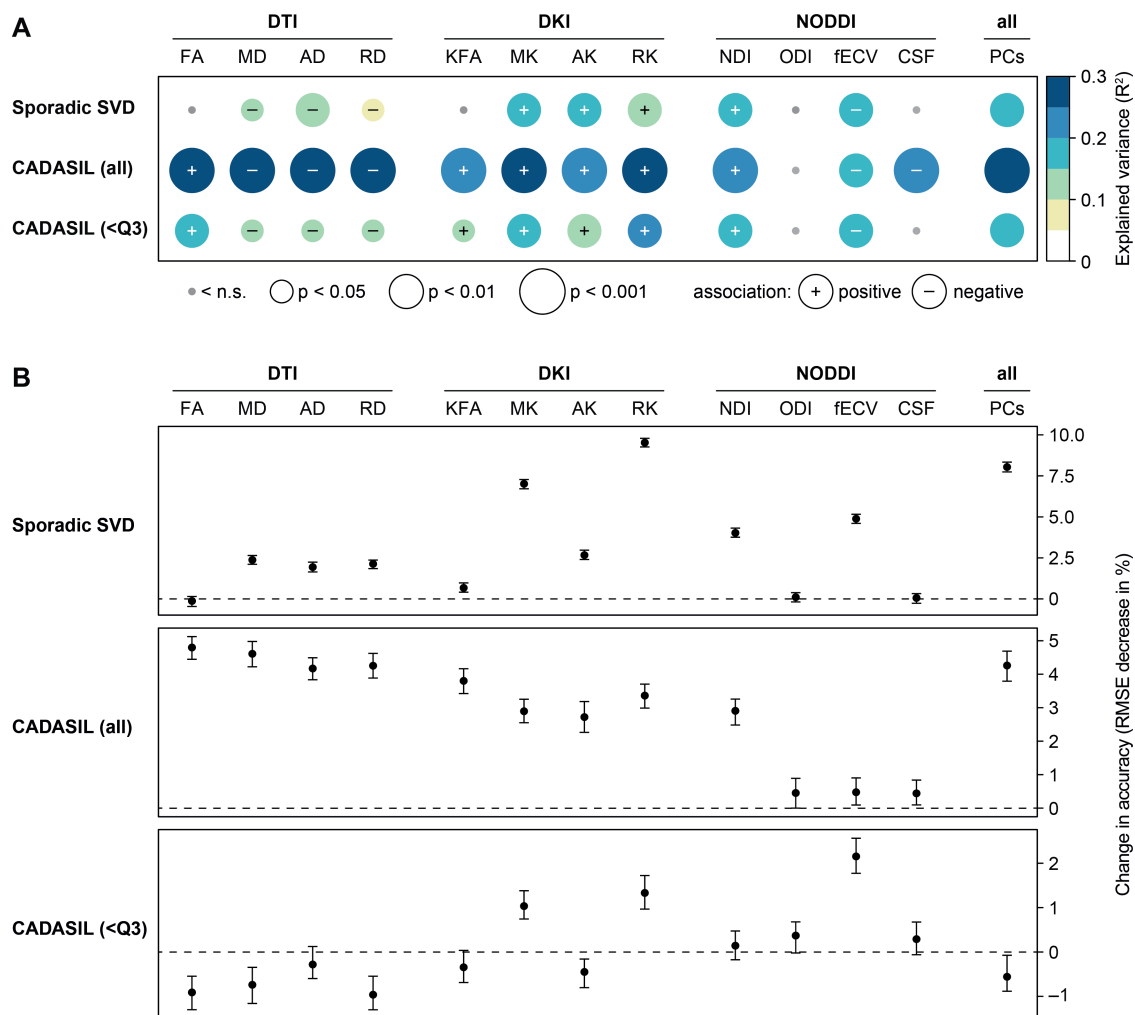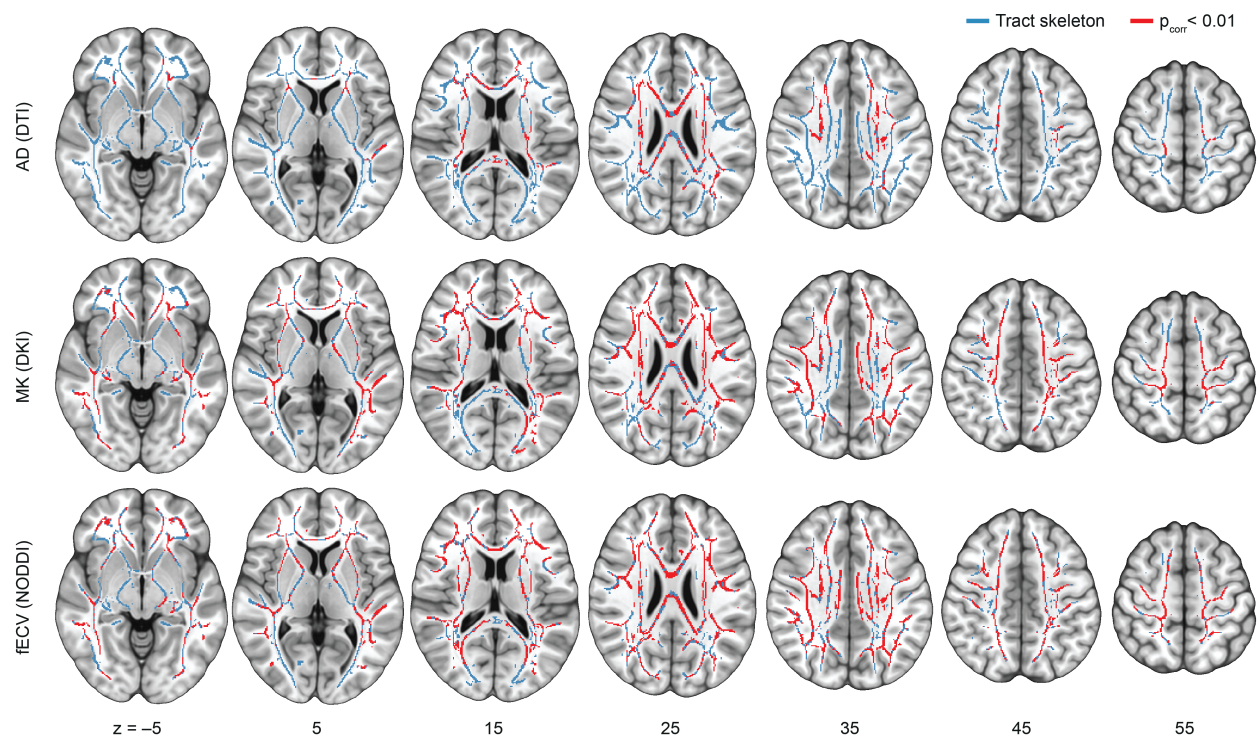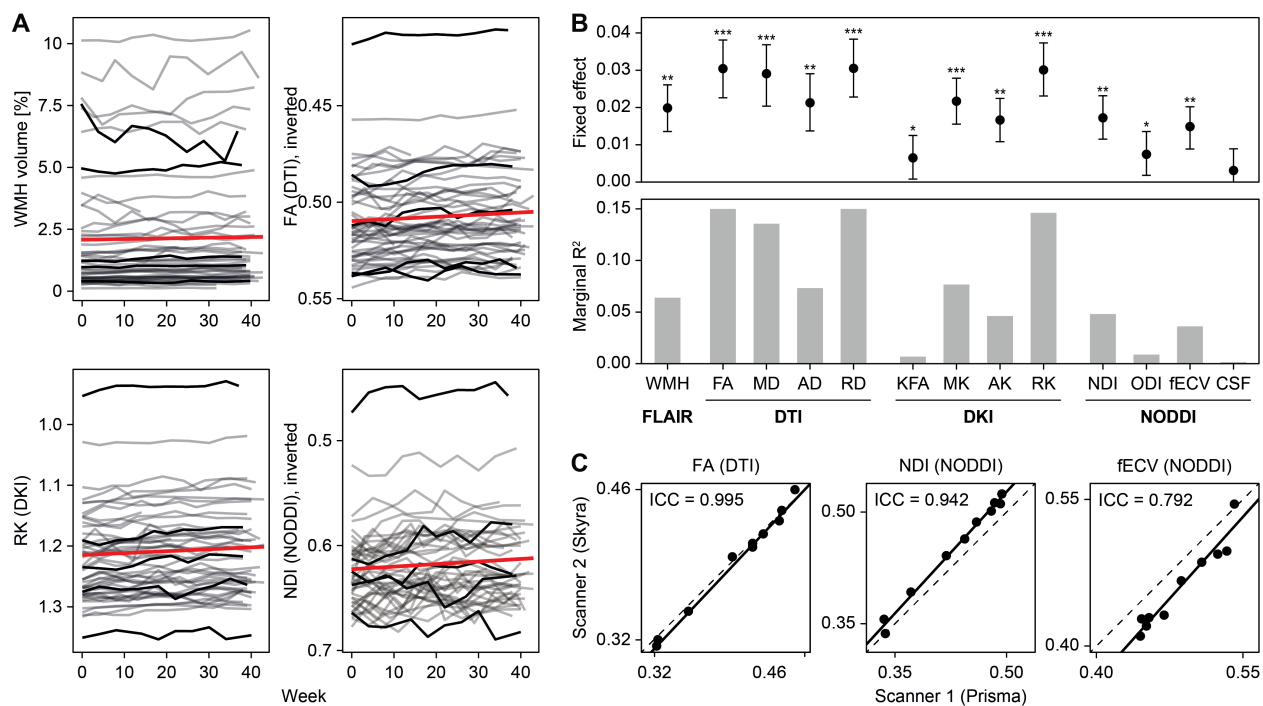
Figure 1

Figure 2

Figure 3

Table e-1: MRI acquisition parameters

Sequence	Feature	Sporadic SVD	CADASIL	
	Scanner	Magnetom Prisma	Magnetom Skyra	Magnetom Prisma
	Coil channels	32 (head)	64 (head-neck)	64 (head-neck)
3D-T1	Type	MP2RAGE	MPRAGE	-
	TR [ms]	5500	2500	-
	TE [ms]	3.84	4.37	-
	TI [ms]	700/2500[a]	1100	-
	Flip angle [˚]	7/4[a]	7	-
	Voxel size [mm]	0.85 isotropic	1 isotropic	-
3D-FLAIR	TR [ms]	5000	5000	-
	TE [ms]	394	398	-
	TI [ms]	1800	1800	-
	Voxel size [mm]	0.85 isotropic	1 isotropic	-
3D-GRE	TR [ms]	35	35	-
	TE [ms]	29.5	29.5	-
	Flip angle [˚]	15	15	-
	Voxel size [mm]	0.8 x 0.8 x 2	0.9 x 0.9 x 2	-
MS-DWI	TR [ms]	3220	3800	3200
	TE [ms]	74	104.8	74
	Flip angle [˚]	90	90	90
	In-plane resolution [mm]	1.7 x 1.7	2 x 2	2 x 2
	Slice thickness [mm]	1.7	2	2
	Base resolution (matrix)	130	120	120
	Number of slices	87	75	75
	b-values [s/mm^2]	1000/3000	1000/2000	1000/2000
	Directions (per b-value)	30/60	30/60	30/60
	b=0 [images]	10	10	10
	Receiver bandwidth [Hz/px]	1924	1894	1954
	Parallel imaging acceleration factor	2	2	2
	multi-band acceleration factor	3	3	3

[a] Double inversion

Abbreviations: CADASIL = Cerebral Autosomal Dominant Arteriopathy with Subcortical Infarcts and Leukoencephalopathy; FLAIR = fluid-attenuated inversion recovery; GRE = gradient echo; MP(2)RAGE = magnetization prepared (2) rapid acquisition gradient echo(es); MS-DWI = multi shell diffusion-weighted imaging; SVD = small vessel disease; TE = echo time; TI = inversion time; TR = repetition time.

Table e-2: Diffusion models and metrics

Model	Metric		Modelled diffusion property/ Microstructural tissue feature
DTI	FA	Fractional anisotropy	Directionality of water diffusion
	MD	Mean diffusivity	Extent of water diffusion
	AD	Axial diffusivity	Extent of water diffusion along the main direction of water diffusion
	RD	Radial diffusivity	Extent of water diffusion perpendicular to the main direction
DKI	KFA	Kurtosis fractional anisotropy	Directionality of kurtosis (i.e. non-Gaussian water diffusion)
	MK	Mean kurtosis	Extent of kurtosis
	AK	Axial kurtosis	Extent of kurtosis parallel to main direction of diffusion
	RK	Radial kurtosis	Extent of kurtosis perpendicular to main direction of diffusion
NODDI	NDI	Neurite density index	Intracellular water content (fraction), modelled as sticks
	ODI	Orientation dispersion index	Angular variation of neurite orientation
	fECV	Extracellular volume fraction	Extracellular water content (fraction), modelled as anisotropic tensor
	fCSF	CSF volume fraction	CSF content (fraction), modelled as isotropic tensor

Abbreviations: CSF = cerebrospinal fluid; DKI = diffusion kurtosis imaging; DTI = diffusion tensor imaging; NODDI = neurite orientation dispersion and density imaging.

Table e-3: Tract-based spatial statistics

	DTI				DKI				NODDI			
	FA	MD	AD	RD	KFA	MK	AK	RK	NDI	ODI	fECV	fCSF
n	0	22016	16643	16969	0	59068	39832	48524	53760	0	55530	0
%	0	26	19	20	0	69	46	57	63	0	65	0

n = number of significant voxels (within the white matter skeleton)

% = percentage of significant voxels in relation to all voxels of the white matter skeleton

Table e-4: Inter-site reproducibility

	DTI				DKI				NODDI			
	FA	MD	AD	RD	KFA	MK	AK	RK	NDI	ODI	fECV	fCSF
ICC	0.995	0.993	0.992	0.993	0.975	0.985	0.931	0.993	0.942	0.255	0.792	0.808

Abbreviations: ICC = intraclass correlation coefficient.